5-HT₃ Receptor Brain-Type B-Subunits are Differentially Expressed in Heterologous Systems

Jeremias Corradi,[†,§] Andrew J. Thompson,[‡,§] Ian McGonigle,[‡] Kerry. L. Price,[‡] Cecilia Bouzat,[*,†] and Sarah C. R. Lummis[*,‡]

[†]INIBIBB, UNS/CONICET, Camino La Carrindanga Km 7, 8000 Bahía Blanca, Argentina
[‡]Department of Biochemistry, University of Cambridge, Cambridge CB2 1QW, United Kingdom

ABSTRACT: Genes for five different 5-HT₃ receptor subunits have been identified. Most of the subunits have multiple isoforms, but two isoforms of the B subunits, brain-type 1 (Br1) and brain-type 2 (Br2) are of particular interest as they appear to be abundantly expressed in human brain, where 5-HT3B subunit RNA consists of approximately 75% 5-HT3Br2, 24% 5-HT3Br1, and <1% 5-HT3B. Here we use two-electrode voltage-clamp, radioligand binding, fluorescence, whole cell, and single channel patch-clamp studies to characterize the roles of 5-HT3Br1 and 5-HT3Br2 subunits on function and pharmacology in heterologously expressed 5-HT₃ receptors. The data show that the 5-HT3Br1 transcriptional variant, when coexpressed with 5-HT3A subunits, alters the EC_{50}, n_H, and single channel conductance of the 5-HT₃ receptor, but has no effect on the potency of competitive antagonists; thus, 5-HT₃ABr1 receptors have the same characteristics as 5-HT₃AB receptors. There were some differences in the shapes of 5-HT₃AB and 5-HT₃ABr1 receptor responses, which were likely due to a greater proportion of homomeric 5-HT₃A versus heteromeric 5-HT₃ABr1 receptors in the latter, as expression of the 5-HT3Br1 compared to the 5-HT3B subunit is less efficient. Conversely, the 5-HT3Br2 subunit does not appear to form functional channels with the 5-HT3A subunit in either oocytes or HEK293 cells, and the role of this subunit is yet to be determined.

KEYWORDS: Serotonin, cys-loop, heteromeric, single channel
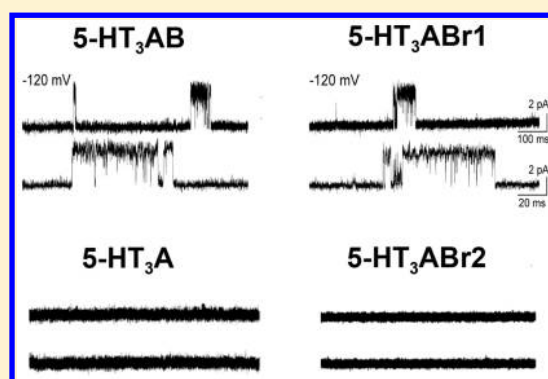
5-HT₃ receptors are members of the Cys-loop family of ligand-gated ion channels that are responsible for fast excitatory and inhibitory synaptic transmission in the central and peripheral nervous systems. Other members of this family include the nACh, GABA, and glycine receptors, all of which share a common structural arrangement and are targets for a range of clinically important drugs.[1−4]

Cys-loop receptors consist of five subunits that surround a central ion-conducting pore. Each subunit can be divided into three functionally distinct regions that are termed the intracellular, transmembrane, and extracellular domains. The intracellular domain, whose structure is not yet known, is responsible for post-translational modulation by intracellular molecules and plays a role in channel conductance.[3,5] The transmembrane domain consists of four membrane-spanning α-helices (M1−M4); M2 lines the pore, enabling ions to pass through the channel. In 5-HT₃ receptors, the pore is cation selective, and its opening results in a rapidly activating and then desensitizing inward current that depolarizes the cell. The extracellular domain contains the ligand binding sites for agonist and competitive antagonists and these are formed by the convergence of six amino acid loops at the interface of two adjacent subunits. Three loops (A−C) arise from the principal subunit and three (D−F) from the complementary subunit. The amino acids responsible for interacting with ligands vary

according to the ligand and receptor being studied, but all binding pockets possess three to five aromatic residues that contribute to an "aromatic box" which is important for binding ligands.

To date, genes for five 5-HT₃ receptor subunits have been identified (5-HT3A−5-HT3E) in humans.[6] Only 5-HT3A subunits can form functional homomeric receptors, and the structure of the mouse 5-HT₃A receptor has recently been solved to high resolution.[7] The other subunits can combine with 5-HT3A to form heteromeric complexes, but, apart from receptors expressing 5-HT3A and 5HT3B subunits (5-HT₃AB receptors), these have not been extensively investigated.[8−10] Most of the subunits have multiple isoforms, but two isoforms of the 5-HT3B subunits, brain-type 1 and brain-type 2 (called here 5-HT3Br1 and 5-HT3Br2 rather than 5-HT3BBr1/2), are of particular interest as their RNAs are abundantly expressed in human brain.[11] These authors reported that in brain less than 1% of the 5-HT3B subunit RNA coded for the conventional 5-HT3B subunit, while the remaining B-subunit RNA was
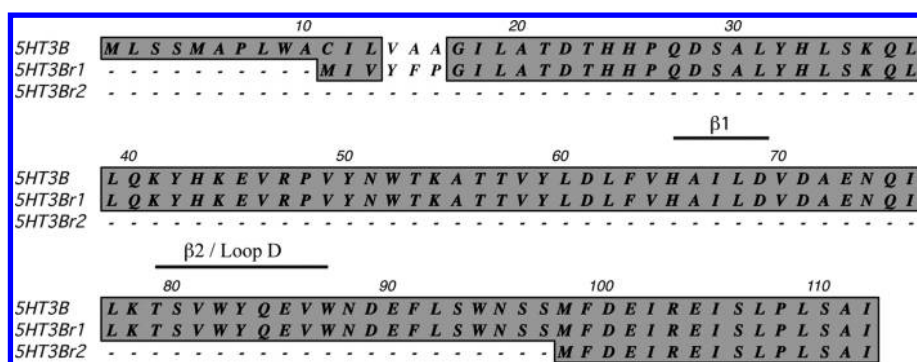
Figure 1. Alignment of the N-terminal region of 5-HT3B, 5-HT3Br1, and 5-HT3Br2 subunits. 5HT3Br1 subunits differ from 5-HT3B subunits only in the extreme N-terminus, while 5HT3Br2 has ∼100 fewer amino acids and is missing the β1 and β2/loop D regions. Differences in the subunits are due to alternative splicing so the remaining sequences are identical.

accounted for by approximately 75% 5-HT3Br2 and 24% 5-HT3Br1. There is therefore the potential that 5-HT$_3$AB receptors in the brain have distinct properties to those in other regions. As 5-HT$_3$ receptor-selective agents have a range of therapeutic applications it is important to better understand the consequences of incorporating these subunits on the pharmacology and physiology of these receptors.

The aim of this study was to assess the functional role of 5-HT$_3$AB receptors containing 5-HT3Br1 or 5-HT3Br2 subunits, which differ only in their N-terminal sequences (Figure 1) compared to the originally described 5-HT3B subunit. We do this using a combination of two-electrode voltage-clamp, radioligand binding, fluorescence, and whole cell and single channel patch-clamp studies.

■ RESULTS AND DISCUSSION

Characterization of 5-HT$_3$A and 5-HT$_3$AB Receptors. Application of 5-HT to *Xenopus* oocytes expressing homomeric or heteromeric receptors produced rapidly activating inward currents that desensitized over the time-course of the application (Figure 2). The shape of the responses elicited by
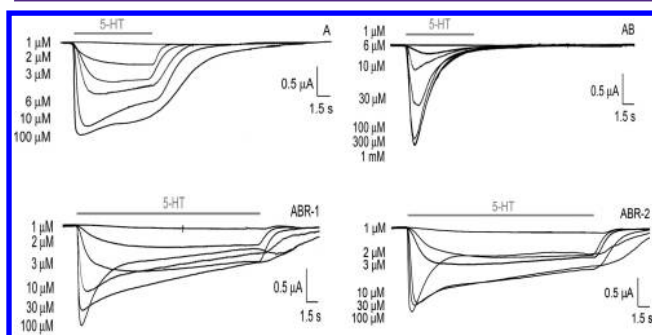

Figure 2. Traces of macroscopic currents from 5-HT$_3$ receptors expressed in oocytes measured using voltage clamp electrophysiology. Typical examples of current traces over a range of 5-HT concentrations for 5-HT$_3$A, 5-HT$_3$AB, 5-HT$_3$ABr1, and 5-HT$_3$ABr2 receptors from the same batch of oocytes are shown. There are distinct differences in the shapes of all the currents.

5-HT$_3$A and 5-HT$_3$AB receptors differed due to faster desensitization of the latter. Concentration−response curves for 5-HT$_3$A and 5-HT$_3$AB receptors also showed differences in 5-HT EC$_{50}$, which was increased in 5-HT$_3$AB compared to 5-HT$_3$A receptors, and Hill slope, which was reduced (Table 1, Figure 2) as previously published.[8−10] Similar differences in

Table 1. Parameters Derived from 5-HT-Induced Macroscopic Responses of 5-HT$_3$ Receptors Expressed in Oocytes

receptor	pEC$_{50}$ (M) mean ± SEM	n_H	n
5-HT$_3$A	5.76 ± 0.02	2.6	6
5-HT$_3$AB	4.55 ± 0.04[a]	1.0	7
5-HT$_3$ABr1	5.09 ± 0.06[a]	1.0	8
5-HT$_3$ABr2	5.48 ± 0.04[b]	1.9	6

[a]Significantly different from 5-HT$_3$A receptors, $p < 0.05$. [b]Significantly different from 5-HT$_3$AB receptors, $p < 0.05$

EC$_{50}$ and n_H were observed for receptors expressed in HEK293 cells, with functional responses measured using a fluorescent membrane potential sensitive dye; EC$_{50}$ was increased and n_H decreased in 5-HT$_3$AB compared to 5-HT$_3$A receptors. Here again there were differences in the shape of the responses: 5-HT$_3$A receptor responses peaked and returned toward baseline over the course of the experiment, while 5-HT$_3$AB responses peaked more slowly and only decreased toward baseline at lower 5-HT concentrations (Figure 3).

Characterization of 5-HT$_3$ABr1 Receptors in Oocytes. Coexpression of 5-HT3Br1 with 5-HT3A subunits produced currents in *Xenopus* oocytes with concentration−response parameters that were similar to 5-HT$_3$AB receptors. This was expected as the amino acid composition of the 5-HT3Br1
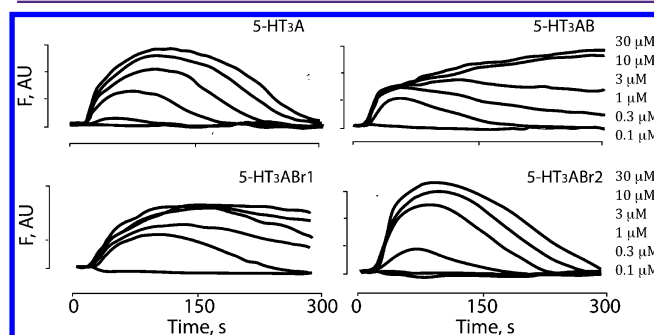

Figure 3. Responses from 5-HT$_3$ receptors expressed in HEK293 cells measured using a fluorescent membrane potential sensitive dye. Typical examples of 5-HT-induced responses over a range of 5-HT concentrations for 5-HT$_3$A, 5-HT$_3$AB, 5-HT$_3$ABr1, and 5-HT$_3$ABr2 receptors are shown. The response profiles of 5-HT$_3$A and 5-HT$_3$AB receptors are different, with 5-HT$_3$ABr1 receptor responses similar to 5-HT$_3$AB receptor responses, and 5HT$_3$Br2 receptor responses similar to 5-HT$_3$A receptor responses. F = arbitrary fluorescent units.

Table 2. Parameters Derived from 5-HT$_3$ Receptors Expressed in HEK293 Cells Using a Membrane Potential Dye or Radioligand Binding[a]

	parameters from functional data		
receptor	pEC$_{50}$ (M)	n_H	K_d (nM) from [^{3}H]granisetron binding data
5-HT$_3$A	6.56 ± 0.02	3.6 ± 0.8	0.33 ± 0.02
5-HT$_3$AB	5.81 ± 0.06[b]	1.3 ± 0.2[b]	0.25 ± 0.08
5-HT$_3$ABr1	5.79 ± 0.08[b]	1.5 ± 0.3[b]	0.35 ± 0.09
5-HT$_3$ABr2	6.43 ± 0.06[c]	2.9 ± 0.4[c]	0.41 ± 0.11

[a]Data = mean ± SEM, $n = 3–8$. [b]Significantly different from 5-HT$_3$A receptors, $p < 0.05$. [c]Significantly different from 5-HT$_3$AB receptors, $p < 0.05$

subunit is very similar to that of the 5-HT3B subunit, with the only difference being a region at the extreme N-terminus of the subunit (Figure 1). This region is likely to be predominantly, if not solely, part of the signal sequence, and thus is not likely to be expressed in the mature protein. However, the shape of the responses in 5-HT$_3$ABr1 receptors differed from those in 5-HT$_3$AB receptors, being somewhat intermediate between those of 5-HT$_3$A and 5-HT$_3$AB receptors (Figure 2), with fast desensitization at high 5-HT concentration but slower desensitization at low concentrations. These differences likely arise as these cells can express both homomeric (5-HT$_3$A) and heteromeric receptors (5-HT$_3$AB/Br1), and the proportions of these may differ depending on which B subunit is being expressed. It is also possible that differential B subunit expression could cause different stoichiometries, and different characteristics, as is the case in certain nACh receptors,[12] although there is currently no evidence for this.

Characterization of 5-HT$_3$ABr1 Receptors in HEK Cells. Coexpression of 5-HT3A and 5-HT3Br1 subunits in HEK cells analyzed using membrane potential fluorescent dye revealed shapes of 5-HT-induced responses that were not significantly different to those of 5-HT$_3$AB receptors (Figure 3). The 5-HT$_3$ABr1 concentration−response curves were right shifted and had lower Hill slopes when compared to 5-HT$_3$A receptors, consistent with voltage clamp measurements in oocytes (Table 2).

The 5-HT3Br1 subunit, however, was expressed and/or incorporated into functional receptors over a different time course and concentration range when compared to the 5-HT3B subunit: higher concentrations and a longer period after transfection were needed to obtain similar effects. Figure 4 shows the effects on receptor parameters determined 2 or 3 days post transfection. Analysis of data obtained 2 days post transfection with 2 or 20 ng 5-HT3B subunit cDNA (both combined with 20 ng 5-HT3A subunit cDNA) revealed receptor characteristics that were consistent with 5-HT$_3$AB receptors, but such characteristics were not apparent in cells transfected with 5-HT3Br1 subunit cDNA until at least 3 days post transfection and required >20 ng 5-HT3Br1 subunit cDNA. These data show that the signal sequence has a significant effect on expression and/or subsequent incorporation of the 5-HT3Br1 subunit into functional receptors, and support the expression hypothesis proposed above (different relative expression levels of homomeric and heteromeric receptors) to explain the different traces in 5-HT$_3$AB and 5-HT$_3$ABr1 receptors. Given these data, a study of the levels of expression of the 5-HT3Br1 subunit protein in brain tissues would be worthwhile, as the data showing high levels of 5-HT3Br1 subunit RNA in neurones may not provide an accurate picture of the relative proportions of different types of 5-HT$_3$ receptor subunits being expressed.
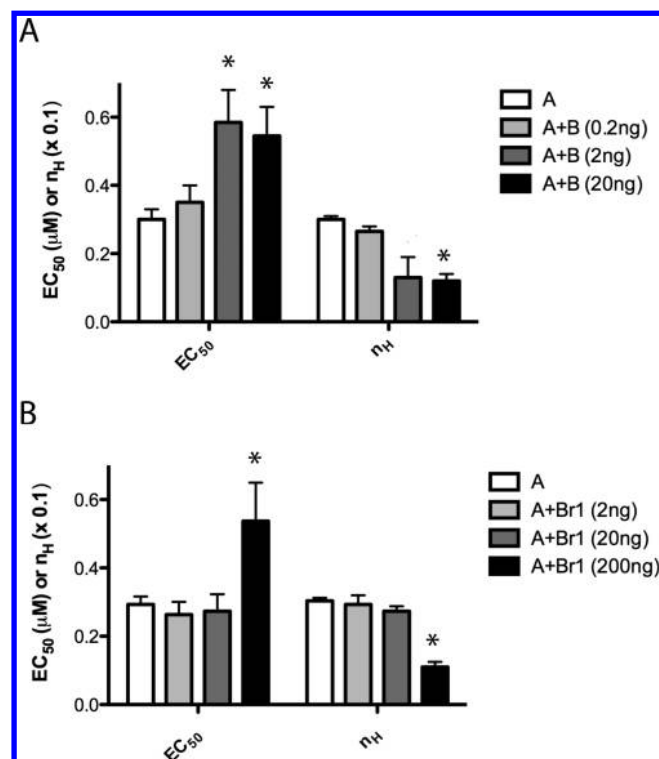

Figure 4. Appearance of 5-HT$_3$AB receptor characteristics differ following transfection with 5-HT3B or 5-HT3Br1 subunits. Cells were transfected with 5-HT3A subunit cDNA (20 ng per well) and various amounts of 5-HT3B or 5-HT3Br1 subunit DNA, and incubated for 2 (A) or 3 (B) days. Higher EC$_{50}$ and lower n_H values (i.e., 5-HT$_3$AB receptor characteristics) were observed in cells incubated for 2 days with 2 and 20 ng of 5-HT3B subunit cDNA, but those transfected with 0.2 ng of cDNA had responses with characteristics consistent with homomeric 5-HT$_3$A receptors. Cells transfected with 200 ng of 5-HT3BR1 subunit cDNA had 5-HT$_3$AB receptor characteristics after 3 days of incubation. Responses with characteristics consistent with homomeric 5-HT$_3$A receptors were observed for cells transfected with 2 or 20 ng of cDNA, and for cells incubated for 2 days (data not shown). Data = mean ± SEM, $n = 3–6$;*significantly different from 5-HT$_3$A receptor responses.

Radioligand binding with the 5-HT$_3$−receptor selective antagonist [^{3}H]granisetron revealed no differences in the K_d values of 5-HT$_3$AB and 5-HT$_3$ABr1 receptors, and these were also similar to values from 5-HT$_3$A receptors (Table 2). We also determined K_i values for a range of competitive antagonists, and all competed with similar affinities with a rank order of potency of palonosetron > granisetron > MDL-72222 > mCPBG > d-TC (Figure 5). These data are consistent with previous studies on 5-HT$_3$A and 5-HT$_3$AB receptors that have demonstrated similar antagonist affinities for a range of compounds, despite some biophysical differences between
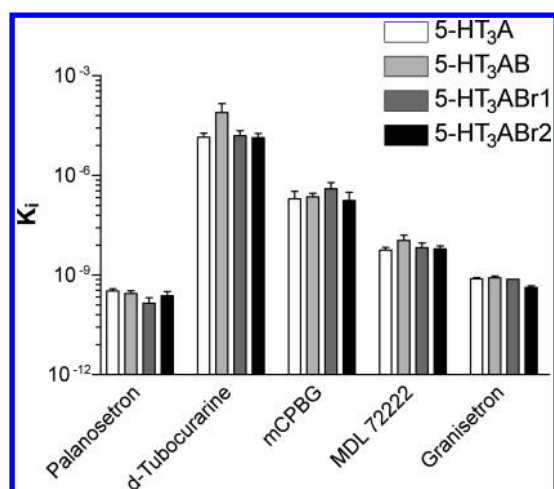
Figure 5. Potencies of ligands at different 5-HT$_3$ receptors expressed in HEK293 cells. The K_i values of a range of competitive 5-HT$_3$ receptor ligands were not significantly different for all the different subtypes. Data = mean ± SEM, $n = 3$−6.

homomeric and heteromeric receptors. This similarity can be readily explained if the binding site for these ligands is at an interface between two adjacent 5-HT3A subunits, which is consistent with the reduced Hill slope of 5-HT concentration−response curve at heteromeric receptors, and our previous findings that mutations to residues in either the principal or complementary face of the 5-HT3B-subunit binding site do not alter ligand binding.[13] Indeed there is good evidence from FRET studies that the orthosteric binding site is located between two adjacent 5-HT3A subunits in both 5-HT$_3$A and 5-HT$_3$AB receptors.[14]

To further probe any differences between 5-HT$_3$AB and 5-HT$_3$ABr1 receptors we explored their single channel currents. Single-channel recordings from cell-attached patches of HEK293 cells expressing 5-HT$_3$AB and 5-HT$_3$ABr1 receptors (1:3 A:B or Br1 ratio) in the presence of 10 μM 5-HT revealed that activation occurred in bursts composed of closely spaced openings separated by brief closed periods. The mean amplitude of single channel openings at −70 mV was 1.95 ± 0.06 pA and 2.17 ± 0.15 pA for 5-HT$_3$AB and 5-HT$_3$ABr1 receptors respectively ($n = 3$), and increased with the decrease of membrane potential (2.9 ± 0.2 and 3.2 ± 0.3 pA, respectively, at −100 mV; Figure 6). The relationship between membrane potential and mean amplitude of the events yielded an estimated conductance of 30 ± 1.2 pS and 33 ± 1.1 pS for 5-HT$_3$AB and 5-HT$_3$ABr1 receptors, respectively (Figure 7). For both receptors, open time histograms were fitted by two exponential components with no significant differences in the mean duration of each component (Figure 6). The mean durations of both components at −100 mV were 3.9 ± 0.9 ms and 0.14 ± 0.05 ms for 5-HT$_3$AB ($n = 6$), and 3.6 ± 0.6 ms and 0.11 ± 0.03 ms for 5-HT$_3$ABr1 ($n = 4$) ($p > 0.1$). In addition, the mean burst duration did not differ between 5-HT$_3$AB (13.5 ± 4.0 ms, $n = 6$) and 5-HT$_3$ABr1 receptors (14.2 ± 5.20 ms, $n = 4$) ($p > 0.1$). Thus, the data show there are no significant differences between single-channel properties of 5-HT$_3$AB and 5-HT$_3$ABr1 receptors.

Characterization of 5-HT$_3$ABr2 Receptors in Oocytes. The shape of the responses in oocytes following coinjection of mRNA for 5-HT3A and 5-HT3Br2 subunits was again somewhat intermediate between those of 5-HT$_3$A and 5-HT$_3$AB receptors, although parameters obtained from concentration−response curves were not significantly different to
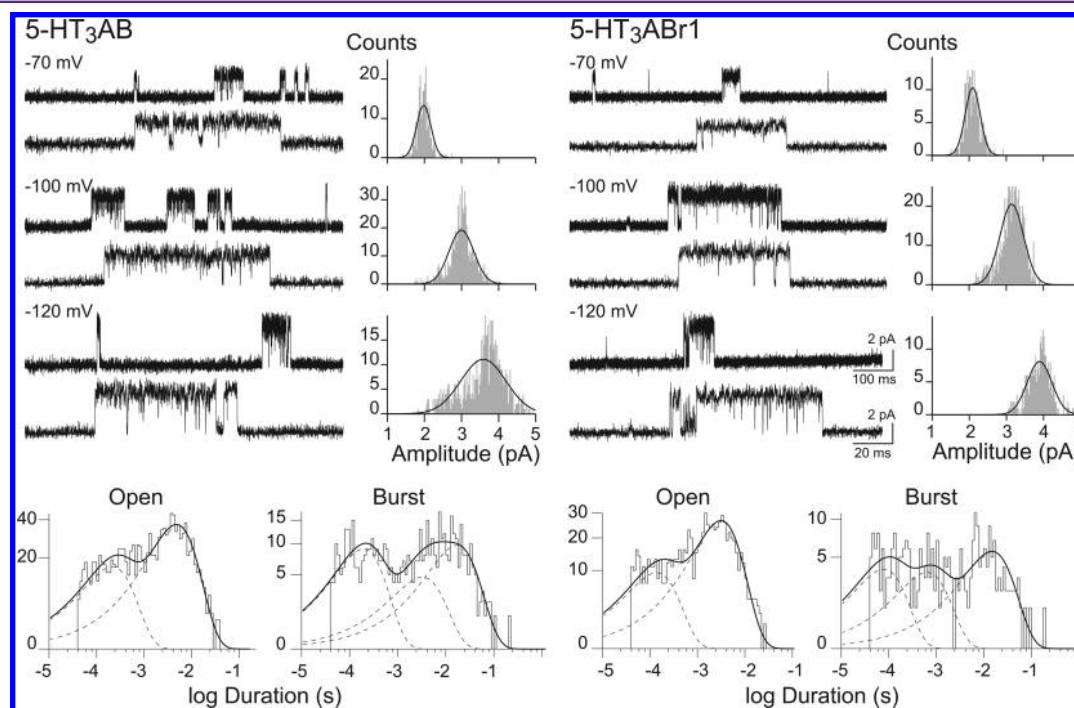

Figure 6. Single-channel currents of 5-HT$_3$AB and 5-HT$_3$ABr1 receptors expressed in HEK293 cells. Single channels activated by 10 μM 5-HT were recorded from cells transfected with 5-HT3A together with 5-HT3B or 5-HT3Br1 subunits (1:3 A:B or Br1 ratio; total DNA, 4 μg/dish). Recordings were made 3 days after transfection. Channels are shown as upward deflections at different membrane potentials and two different temporal scales for each receptor. Filter: 10 kHz. Representative amplitude histograms at different membrane potentials are shown. At the bottom, representative open- and burst-duration histograms for each receptor at −100 mV are shown.
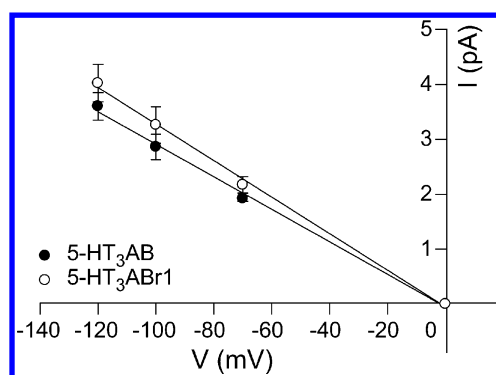
Figure 7. Current−voltage (IV) relationships for 5-HT$_3$AB and 5-HT$_3$ABr1 receptors expressed in HEK293 cells. Data corresponds to the mean amplitude (I) ± SD for at least 160 opening events from three different cells, transfected as in Figure 6, for each condition. The mean amplitude was obtained from the corresponding amplitude histogram. The conductance was obtained from the slope of the curve. Data are not significantly different ($p > 0.05$).

those obtained from 5-HT$_3$A receptors. These data could indicate that the 5-HT3Br2 subunit is being incorporated into receptors, but has no effect on receptor parameters. To test this, we examined the potency of picrotoxinin. This compound acts in the pore and has differing potencies at 5-HT$_3$A and 5-HT$_3$AB receptors (IC$_{50}$s of 11 and 62 μM respectively) due to the different pore lining residues contributed by the 5-HT3B (and similarly the 5-HT3Br1 and 5-HT3Br2) subunits.[15] Here picrotoxinin had an IC$_{50}$ of 17 μM (pIC$_{50}$ = 4.77 ± 0.14, n = 3), which is not significantly different from the value obtained for 5-HT$_3$A receptors (pIC$_{50}$ = 4.97 ± 0.12, n = 13), suggesting the 5-HT3Br2 subunit was not part of the functional receptor.

Characterization of 5-HT$_3$ABr2 Receptors in HEK Cells. Coexpression of 5-HT$_3$A and 5-HT$_3$Br2 receptor subunits in HEK cells analyzed using membrane potential fluorescent dye revealed concentration response parameters and shapes of traces that were indistinguishable from those of 5-HT$_3$A receptors (Figure 3). Macroscopic currents measured in the whole cell configuration from cells transfected with 5-HT3A and 5-HT3Br2 subunits (1:9 ratio) were similar to those of 5-HT$_3$A receptors and clearly different to those of 5-HT$_3$AB receptors (Figure 8).

Moreover, despite the detection of whole-cell macroscopic currents in 5-HT$_3$ABr2 transfected cells, no single channel events were detected in 30 different patches from green cells and two different transfections (ratios 1:3 and 1:9 of 5-HT3A:5-HT3Br2 subunits) (Figure 8). These data are therefore consistent with functional expression of solely homomeric 5-HT$_3$A receptors, whose conductance is too low to allow detection of single channel openings.[16] It has been shown that only after the introduction of the triple QDA mutation at determinants of ion conductance of the 5-HT3A subunit, which mimics the amino acids found in the 5-HT3B subunit, single-channel openings of 5-HT$_3$A receptors can be detected under the present recording conditions.[16−18] Incorporation of even one 5-HT3Br2 subunit into receptors should permit the detection of such events, as this subunit possesses the high-conductance triple QDA motif that can be readily detected even when only a single subunit is present.[19,20]

This apparent lack of incorporation of the 5-HT3Br2 subunit into functional heteromeric receptors is likely to be due to its unusual sequence: this subunit is missing the $\beta1$-$\beta2$ loop and
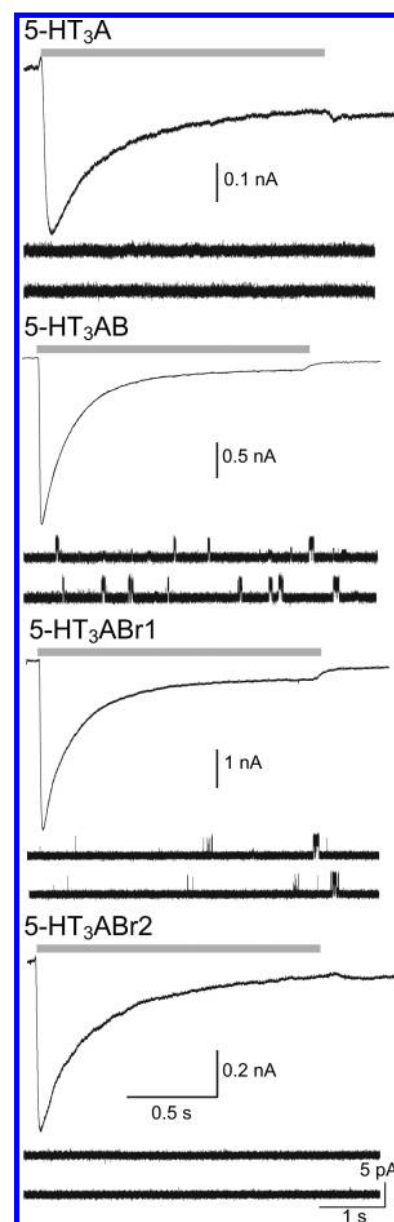

Figure 8. Macroscopic and single-channel recordings from HEK293 cells cotransfected with 5-HT3A or in combination with 5-HT3B, 5-HT3Br1, or 5-HT3Br2 subunits. Representative traces of macroscopic (top of each panel) and single-channel currents (bottom of each panel) from cells transfected with only 5-HT3A or together with 5-HT3Br2 or 5-HT3B subunits are shown (subunit ratio 1:3 for A:B and A:Br1, and 1:9 for A:Br2, total DNA was 4 μg/dish). Macroscopic currents were recorded in the whole cell configuration at a holding potential of −50 mV and were elicited by a pulse of 100 μM 5-HT (gray bar). Single-channel currents were recorded from cell-attached patches at −100 mV in the presence of 10 μM 5-HT. Channel openings are shown as upward deflections.

loop D, which are essential for gating.[21] The considerable abundance of 5-HT$_3$Br2 mRNA in the brain, however, suggests it is important.[11] This subunit may therefore have some other role, and warrants further investigation.

■ CONCLUSION

This study demonstrates that the 5-HT3Br1 transcriptional variant of the 5-HT3B subunit can contribute to the functional properties of heteromeric receptors in a similar manner to the

originally characterized 5-HT3B subunit, altering the EC_{50}, n_H, and single channel conductance of the 5-HT$_3$A receptor. Its expression levels, however, differ significantly from those of the canonical 5-HT3B subunits in heterologous systems. Conversely the 5-HT3Br2 subunit does not form functional channels with the 5-HT3A subunit in either oocytes or HEK cells. Its physiological role is yet to be determined.

■ METHODS

Materials. All cell culture reagents were obtained from Gibco (Invitrogen Ltd., Paisley, U.K.), except fetal calf serum which was from Labtech International (Ringmer, U.K.). Human 5-HT$_3$A (accession number: P46098) and 5-HT$_3$B (O95264) receptor subunit cDNA was kindly gifted by Prof J. A. Peters (University of Dundee, U.K.). 5-HT3Br1 and 5-HT3Br2 subunit cDNAs were generated by Quikchange mutagenesis.

Oocyte Maintenance. *Xenopus laevis* oocyte-positive females were purchased from NASCO (Fort Atkinson, WI) and maintained according to standard methods. Harvested stage V–VI *Xenopus* oocytes were washed in four changes of Ca-free ND96 (96 mM NaCl, 2 mM KCl, 1 mM MgCl$_2$, 5 mM HEPES, pH 7.5), defolliculated in 1.5 mg mL^{-1} collagenase Type 1A for approximately 2 h, washed again in four changes of ND96, and then stored in ND96 containing 2.5 mM sodium pyruvate, 50 mM gentamycin, and 0.7 mM theophylline.

HEK293 Cell Culture. Human embryonic kidney (HEK) 293 cells were maintained on 90 mm tissue culture plates at 37 °C and 7% CO$_2$ in a humidified atmosphere. They were cultured in DMEM:F12 with GlutaMAX I media (Dulbecco's modified Eagle's Medium/Nutrient Mix F12 (1:1), Invitrogen, Paisley, U.K.) containing 10% fetal calf serum. Cells in 90 mm dishes were transfected using polyethylenimine (PEI). Then 30 μL of PEI (1 mg/mL), 4 μL of cDNA (1 mg/mL) and 1 mL of DMEM were incubated for 10 min at room temperature, added dropwise to a 80–90% confluent plate, and incubated for 2–3 days. For Flexstation studies, cells were transferred to 96-well plates and allowed to adhere overnight before use.

Receptor Expression. cDNA was cloned into pGEMHE for oocyte expression, and pcDNA3.1 (Invitrogen, Paisley, U.K.) for expression in HEK 293 cells. Mutagenesis (Figure 1) was performed using QuikChange (Agilent Technologies Inc., Santa Clara, CA). cRNA was in vitro transcribed from linearized pGEMHE cDNA template using the mMessage mMachine T7 Transcription kit (Ambion, Austin, TX). 5-HT3A was linearized with SphI and 5-HT3B cDNA with NheI. Stage V and VI oocytes were injected with 50 nL of ~400 ng μL^{-1} cRNA, and currents were recorded 1–4 days postinjection. Ratios of 1:3 (5-HT3A:5-HT3B/5-HT3Br1/5-HT3Br2) were used for the expression of heteromeric receptors unless otherwise stated. These levels were previously found to be optimal for 5-HT$_3$AB receptor expression, as ratios ≤1:1 resulted in more 5-HT$_3$A receptor-like responses and ≥1:10 showed poorer total receptor expression.

Fluorometric Analysis. This was as previously described.[22] In brief, fluorescent membrane potential dye (Membrane Potential Blue kit, Molecular Devices) was diluted in Flex buffer (10 mM HEPES, 115 mM NaCl, 1 mM KCl, 1 mM CaCl$_2$, 1 mM MgCl$_2$, and 10 mM glucose, pH 7.4) and 100 μL added to each well of transfected cells. The cells were incubated at 37 °C for 45 min, and then fluorescence was measured in a FlexStation (Molecular Devices) at 2 s intervals for 200 s. 5-HT (Sigma) was added to each well after 20 s. Analysis and curve fitting was performed using Prism (GraphPad Software, San Diego, CA, www.graphpad.com).

TEVC Electrophysiology. Using two electrode voltage-clamp, *Xenopus* oocytes were clamped at −60 mV using an OC-725 amplifier (Warner Instruments, Hamden, CT), Digidata 1322A, and the Strathclyde Electrophysiology Software Package (Department of Physiology and Pharmacology, University of Strathclyde, UK). Currents were recorded at a frequency of 5 kHz and filtered at 1 kHz. Microelectrodes were fabricated from borosilicate glass (GC120TF-10, Harvard Apparatus, Edenbridge, Kent, U.K.) using a one stage horizontal pull (P-87, Sutter Instrument Company, Novato, CA) and filled with 3 M KCl. Pipet resistances ranged from 1.0 to 2.0

MΩ. Oocytes were perfused with saline at a constant rate of 12 mL min^{-1}. Drug application was via a simple gravity fed system calibrated to run at the same rate. Extracellular saline contained (mM), 96 NaCl, 2 KCl, 1 MgCl$_2$, and 5 mM HEPES; pH 7.4 with NaOH).

Concentration–response data for each oocyte was normalized to the maximum current for that oocyte, and analysis and curve fitting was performed using Prism.

Whole-Cell Patch-Clamp Electrophysiology. Macroscopic current recordings were recorded in the whole-cell configuration essentially as described before.[17] For whole-cell recordings, the perfusion system consisted of solution reservoirs, manual switching valves, a solenoid-driven pinch valve, and two tubes (inner diameter, 0.3 mm) oriented at 90° inserted into the culture dish (modified from ref 23). One tube contained extracellular solution (ECS) without agonist (normal solution), and the other contained ECS with of 5-HT (test solution). A series of 1.5 s pulses of ECS containing 100 μM 5-HT were applied at 15 s intervals. The pipet solution contained 134 mM KCl, 5 mM EGTA, 1 mM MgCl$_2$, and 10 mM HEPES, pH 7.3. The extracellular solution contained 150 mM NaCl, 5.6 mM KCl, 0.5 mM CaCl$_2$, and 10 mM HEPES, pH 7.3. Macroscopic currents were recorded at an applied potential of −50 mV, filtered at 5 kHz, and digitized at 20 kHz. Data analysis was performed using the IgorPro software (Wavemetrics). For each experiment, three to five individual records were aligned at the point at which the current reached 50% of maximum, and expressed as their average. The solution exchange time was estimated by placing an open pipet at the cell position, and switching from normal bath solution to a diluted (1:1 with water) bath solution. Typical times varied between 1 and 2 ms.

Single-Channel Patch-Clamp Recordings. Single-channel recordings were obtained in the cell-attached patch configuration essentially as described before.[17] The bath and pipet solutions contained 142 mM KCl, 5.4 mM NaCl, 0.2 mM CaCl$_2$, and 10 mM HEPES, pH 7.4. Single-channel currents were recorded and low-pass filtered to 10 kHz using an Axopatch 200 B patch-clamp amplifier (Molecular Devices), digitized at 5 μs intervals, and detected by the half amplitude threshold criterion using the program TAC (Bruxton Corporation). Open-time histograms were fitted by the sum of exponential functions by maximum likelihood using the program TACFit (Bruxton Corporation). Bursts were identified as a series of closely separated openings (more than five) preceded and followed by closings longer than a critical duration. The critical time was taken as the point of intersection of the second and the third component in the closed-time histogram for bursts (τ_c^b). Typically, τ_c^b were between 0.2 and 0.6 ms. Burst duration was obtained from the longest duration component of the open-time histogram constructed with the critical time for defining bursts.

Radioligand Binding. Transfected HEK 293 cells were scraped into 1 mL of ice-cold HEPES buffer (10 mM, pH 7.4) and frozen. After thawing, they were washed with HEPES buffer and resuspended, and then 50 μg of cell membranes was incubated in 0.5 mL of HEPES buffer containing 1 nM [^{3}H]granisetron ($\sim K_d$) in a total volume of 500 μL. Nonspecific binding was determined using 1 mM quipazine or 10 μM d-tubocurarine, giving the same result. For competition binding (8 point), reactions were incubated for at least 1 h at 4 °C. Reactions were terminated by vacuum filtration using a Brandel cell harvester onto GF/B filters presoaked in 0.3% polyethylenimine. Radioactivity was determined by scintillation counting using a Beckman BCLS6500 instrument (Fullerton, CA). Individual competition binding experiments were analyzed by iterative curve fitting using Prism.

Statistical Analysis. Statistical analysis was performed using Prism using Student's *t* test or one-way ANOVA as appropriate, and $p < 0.05$ was taken as statistically significant.

■ AUTHOR INFORMATION

Corresponding Authors
*E-mail: sl120@cam.ac.uk.
*E-mail: inbouzat@criba.edu.ar.

Author Contributions

§J.C. and A.J.T. contributed equally to this work. Participated in research design: S.C.R.L., C.B., A.J.T., I.M., and J.C. Conducted experiments: I.M., J.C., A.J.T., and S.C.R.L. Performed data analysis: J.C., I.M., C.B., A.J.T., and S.C.R.L. Wrote or contributed to the writing of the manuscript: S.C.R.L., A.J.T., and C.B.

Notes

The authors declare no competing financial interest.

■ ACKNOWLEDGMENTS

■ ABBREVIATIONS

5-HT, 5-hydroxytryptamine; nACh receptor, nicotinic acetylcholine; GABA, gamma-aminobutyric acid; HEK, human embryonic kidney; AChBP, acetylcholine binding protein

■ REFERENCES

(1) Johnston, G. A. (2005) $GABA_A$ receptor channel pharmacology. *Curr. Pharm. Des. 11* (15), 1867−1885.

(2) Lummis, S. C. (2012) 5-HT$_3$ receptors. *J. Biol. Chem. 287* (48), 40239−40245.

(3) Thompson, A. J., Lester, H. A., and Lummis, S. C. (2010) The structural basis of function in Cys-loop receptors. *Q. Rev. Biophys. 43* (4), 449−499.

(4) Webb, T. I., and Lynch, J. W. (2007) Molecular pharmacology of the glycine receptor chloride channel. *Curr. Pharm. Des. 13* (23), 2350−2367.

(5) Kelley, S. P., Dunlop, J. I., Kirkness, E. F., Lambert, J. J., and Peters, J. A. (2003) A cytoplasmic region determines single-channel conductance in 5-HT$_3$ receptors. *Nature 424* (6946), 321−324.

(6) Niesler, B., Walstab, J., Combrink, S., Moller, D., Kapeller, J., Rietdoorf, J., Bonisch, H., Gothert, M., Rappold, G., and Bruss, M. (2007) Characterization of the novel human serotonin receptor subunits 5-HT3C, 5-HT3D, and 5-HT3E. *Mol. Pharmacol. 72*, 8−17.

(7) Hassaine, G., Deluz, C., Grasso, L., Wyss, R., Tol, M. B., Hovius, R., Graff, A., Stahlberg, H., Tomizaki, T., Desmyter, A., Moreau, C., Li, X. D., Poitevin, F., Vogel, H., and Nury, H. (2014) X-ray structure of the mouse serotonin 5-HT$_3$ receptor. *Nature 512*, 276−281.

(8) Brady, C. A., Stanford, I. M., Ali, I., Lin, L., Williams, J. M., Dubin, A. E., Hope, A. G., and Barnes, N. M. (2001) Pharmacological comparison of human homomeric 5-HT$_3$A receptors versus heteromeric 5-HT3A/3B receptors. *Neuropharmacology 41* (2), 282−284.

(9) Davies, P. A., Pistis, M., Hanna, M. C., Peters, J. A., Lambert, J. J., Hales, T. G., and Kirkness, E. F. (1999) The 5-HT3B subunit is a major determinant of serotonin-receptor function. *Nature 397* (6717), 359−363.

(10) Thompson, A. J., and Lummis, S. C. (2013) Discriminating between 5-HT$_3$A and 5-HT$_3$AB receptors. *Br. J. Pharmacol. 169* (4), 736−747.

(11) Tzvetkov, M. V., Meineke, C., Oetjen, E., Hirsch-Ernst, K., and Brockmoller, J. (2007) Tissue-specific alternative promoters of the serotonin receptor gene HTR3B in human brain and intestine. *Gene 386* (1−2), 52−62.

(12) Bermudez, I., and Moroni, M. (2006) Phosphorylation and function of alpha4beta2 receptor. *J. Mol. Neurosci 30*, 97−98.

(13) Thompson, A. J., Price, K. L., and Lummis, S. C. (2011) Cysteine modification reveals which subunits form the ligand binding site in human heteromeric 5-HT$_3$AB receptors. *J. Physiol. 589* (Pt 17), 4243−4257.

(14) Miles, T. F., Dougherty, D. A., and Lester, H. A. (2011) The 5-HT$_3$AB receptor shows an A3B2 stoichiometry at the plasma membrane. *Biophys. J. 105*, 887−898.

(15) Thompson, A. J., Duke, R. K., and Lummis, S. C. (2011) Binding sites for bilobalide, diltiazem, ginkgolide, and picrotoxinin at the 5-HT$_3$ receptor. *Mol. Pharmacol. 80* (1), 183−190.

(16) Bouzat, C., Bartos, M., Corradi, J., and Sine, S. M. (2008) The interface between extracellular and transmembrane domains of homomeric Cys-loop receptors governs open-channel lifetime and rate of desensitization. *J. Neurosci. 28*, 7808−7819.

(17) Corradi, J., Gumilar, F., and Bouzat, C. (2009) Single-channel kinetic analysis for activation and desensitization of homomeric 5-HT$_3$A receptors. *Biophys. J. 97* (5), 1335−1345.

(18) Corradi, J., Gumilar, F., and Bouzat, C. (2009) Unraveling Mechanisms Underlying Partial Agonism in 5-HT$_3$A Receptors. *J. Neurosci. 34*, 16865−16876.

(19) Andersen, N., Corradi, J., Sine, S. M., and Bouzat, C. (2013) Stoichiometry for activation of neuronal alpha7 nicotinic receptors. *Proc. Natl. Acad. Sci. U. S. A. 110*, 20819−20824.

(20) Rayes, D., De Rosa, M. J., Sine, S. M., and Bouzat, C. (2009) Number and locations of agonist binding sites required to activate homomeric Cys-loop receptors. *J. Neurosci. 29* (18), 6022−6032.

(21) Reeves, D. C., Jansen, M., Bali, M., Lemster, T., and Akabas, M. H. (2005) A role for the beta 1-beta 2 loop in the gating of 5-HT$_3$ receptors. *J. Neurosci. 25* (41), 9358−9366.

(22) Price, K. L., and Lummis, S. C. (2005) FlexStation examination of 5-HT$_3$ receptor function using Ca^{2+}- and membrane potential-sensitive dyes: Advantages and potential problems. *J. Neurosci. Methods 149* (2), 172−177.

(23) Liu, Y., and Dilger, J. P. (1991) Opening rate of acetylcholine receptor channels. *Biophys. J. 60*, 424−432.